Research Article

Myeloid cell plasticity in the evolution of central nervous system autoimmunity

Running head: Myeloid cell plasticity in central autoimmunity

David A. Giles, BS,[1,2,3] Jesse M. Washnock-Schmid, BS,[1] Patrick C. Duncker, BS,[1,2] Somiah Dahlawi, PhD,[4] Gerald Ponath, PhD,[4] David Pitt, MD,[4] and Benjamin M. Segal, MD[1,2,5]

[1]Holtom-Garrett Program in Neuroimmunology, Department of Neurology, University of Michigan, Ann Arbor, MI, USA.

[2]Graduate Program in Immunology, University of Michigan, Ann Arbor, MI, USA.

[3]Medical Scientist Training Program, University of Michigan, Ann Arbor, MI, USA.

[4]Department of Neurology, School of Medicine, Yale University, New Haven, CT, USA.

[5]Neurology Service, VA Ann Arbor Healthcare System, Ann Arbor, MI, USA.

Corresponding author: Benjamin M. Segal

Corresponding author's address: 4013 BSRB, 109 Zina Pitcher Place, Ann Arbor, MI 48109, USA

Corresponding author's phone and fax: 734-615-0036

Corresponding author's e-mail address: bmsegal@umich.edu

Number of characters in title: 79
Number of characters in running head: 47
Number of words in abstract: 249
Number of words in introduction: 500
Number of words in discussion: 620
Number of words in body of manuscript: 4030
Number of figures: 5
Number of tables: 1

This is the author manuscript accepted for publication and has undergone full peer review but has not been through the copyediting, typesetting, pagination and proofreading process, which may lead to differences between this version and the Version of record. Please cite this article as doi:10.1002/ana.25128.

ABSTRACT

Objective: Myeloid cells, including macrophages and dendritic cells, are a prominent component of central nervous system (CNS) infiltrates during multiple sclerosis (MS) and the animal model experimental autoimmune encephalomyelitis (EAE). Although myeloid cells are generally thought to be pro-inflammatory, alternatively-polarized subsets can serve non-inflammatory and/or reparative functions. Here we investigate the heterogeneity and biological properties of myeloid cells during central nervous system autoimmunity. **Methods:** Myeloid cell phenotypes in chronic active MS lesions were analyzed by immunohistochemistry. In addition, immune cells were isolated from the CNS during exacerbations and remissions of EAE and characterized by flow cytometric, genetic and functional assays. **Results:** Myeloid cells expressing iNOS, indicative of a pro-inflammatory phenotype, were detected in the actively demyelinating rim of chronic active MS lesions, whereas macrophages expressing mannose receptor (CD206), a marker of alternatively-polarized human myeloid cells, were enriched in the quiescent lesion core. During EAE, CNS-infiltrating myeloid cells, as well as microglia, shifted from expression of pro- to non-inflammatory markers immediately prior to clinical remissions. Murine CNS myeloid cells expressing the alternative lineage marker arginase-1 (Arg1) were partially derived from $iNOS^+$ precursors and were deficient in activating encephalitogenic T cells compared with their $Arg1^-$ counterparts. **Interpretation:** These observations demonstrate the heterogeneity of CNS myeloid cells, their evolution during the course of autoimmune demyelinating disease, and their plasticity on the single cell level. Future therapeutic strategies for disease modification in individuals with MS may be focused on accelerating the transition of CNS myeloid cells from a pro- to a non-inflammatory phenotype.

INTRODUCTION

Myeloid cells, including macrophages (MΦ) and dendritic cells (DC), are a major component of white matter lesions in multiple sclerosis (MS) and the animal model experimental autoimmune encephalomyelitis (EAE)[1,2]. Our laboratory and others have established a critical role of myeloid cells in early EAE pathogenesis[3–6]. Myeloid cells may serve as antigen presenting cells for re-activation of myelin-specific $CD4^+$ T cells[7,8], secrete cytokines such as IL-6, IL-1β, and TNFα[9], and directly inflict damage through release of toxic factors such as reactive oxygen species generated by inducible nitric oxide synthase (iNOS)[10,11]. iNOS-expressing myeloid cells are often described as classically-activated, and considered "pro-inflammatory", based on their similarity to bone marrow derived macrophages (BMDM) polarized with LPS or IFNγ *in vitro*[12]. It is generally thought that classically-activated myeloid cells (CAMC) are predominant in active MS and EAE lesions where they act as pathogenic effector cells[13–15]. Early studies of autopsied MS brains revealed iNOS-immunoreactive macrophages in active lesions[14,16,17]. The presence of $iNOS^+$ myeloid cells generally correlated with zones of ongoing demyelination.

However, there is growing evidence that myeloid cells that accumulate in the central nervous system (CNS) are heterogeneous and likely encompass a spectrum of lineages with diverse, and even opposing, properties[18–20]. In contrast to iNOS, the enzyme arginase-1 (Arg1) and the mannose receptor CD206 have been identified as markers of myeloid cells with "immunosuppressive" or "pro-regenerative" properties. Arg1/CD206-expressing myeloid cells play a critical role in wound healing[21]. They are frequently classified as alternatively-activated based on their similarity to BMDM generated *in vitro* by polarization with IL-4 or IL-13 via a STAT6-dependent pathway[12,22]. Alternatively-activated myeloid cells (AAMC) may regulate the inflammatory environment by secreting IL-10 and/or TGFβ1[9], while promoting tissue regeneration by clearing debris[23,24] and secreting growth factors[25]. Foamy (lipid-laden) macrophages, perivascular macrophages, and microglia expressing human AAMC markers, such as CD206 and CD163, have been discovered in acute and chronic active MS lesions[2,19,25,26]. Primary human macrophages acquire a foamy morphology and produce immunosuppressive factors following ingestion of myelin *in vitro*[19].

We questioned whether CNS myeloid cells evolve during disease progression and shift from a pro-inflammatory phenotype at onset to a non-inflammatory or immunosuppressive state in anticipation of clinical

remission/stabilization. Consistent with this hypothesis, CNS-infiltrating DC were found to upregulate the AAMC-associated genes *Arg1*, *Chi3l3* and *Ms4a8a* at the peak of EAE, shortly prior to remission[27]. In fact, Arg1 is the most-significantly up-regulated gene in the CNS at peak EAE[28]. Adoptive transfer of AAMC-polarized macrophages or microglia can ameliorate EAE[29,30], and the therapeutic effects of estrogen, glatiramer acetate and other agents in EAE were found to correlate with the expansion of AAMC in the periphery and/or CNS[31–34]. Less is known about endogenous AAMC that spontaneously accumulate in the CNS during the course of EAE or MS. In the current paper, we compare the spatial distribution of AAMC in actively demyelinating and quiescent regions of MS lesions. In addition, we examine the origin, kinetics and biological properties of CNS myeloid subsets from the preclinical stage of EAE through peak and remission.

METHODS

Mice. C57Bl/6 and B6.Ly5.1 mice were from Charles River Laboratories. Arg1-eYFP[35], Rosa-LSL-eYFP, 2D2 TCR transgenic, and STAT6$^{-/-}$ mice were from the Jackson Laboratory. iNOS-TdTomato-Cre[36] mice were from the European Mouse Mutant Archive. SJL mice were from Harlan Laboratory. Both male and female mice, age 6-12 weeks, were used in experiments. All mice were bred and maintained under specific pathogen-free conditions at the University of Michigan, and all animal experiments were performed in accordance with an IACUC-approved protocol at the University of Michigan.

Induction and assessment of EAE. For active immunization, C57Bl/6 mice were subcutaneously immunized over the flanks with 100 µg MOG_{35-55} (Biosythesis) in complete Freund's adjuvant (Difco). Mice were injected intraperitoneally with 300 ng pertussis toxin (List Biological) on days 0 and 2. For adoptive transfer, mice were immunized as described, without pertussis toxin, and the draining lymph nodes (inguinal, brachial, and axillary) were collected at 10-14 days post-immunization. Lymph node cells were cultured for 96 hours in the presence of 50 ug/mL MOG_{35-55}, 8 ng/ml IL-23 (R&D Systems), 10 ng/ml IL-1α (Peprotech), and 10 µg/mL anti-IFNγ (Clone XMG1.2, BioXcell). At the end of culture, $CD4^+$ T cells were purified with CD4 positive selection magnetic beads (Miltenyi), and 3-5x10^6 $CD4^+$ T cells were transferred intraperitoneally into naïve recipients. For induction of relapsing-remitting EAE, SJL mice were subcutaneously immunized over the flanks with 100 µg $PLP_{139-151}$ (Biosynthesis) in complete Freund's adjuvant (Difco) without pertussis toxin. EAE was assessed by a clinical score of disability: 1, limp tail; 2, hind-limb weakness; 3, partial hind-limb paralysis; 4, complete hind-limb paralysis; and 5, moribund state.

Mixed bone marrow chimeras. B6.Ly5.1 ($CD45.1^+$) congenic hosts were lethally irradiated with 1300 Rad split into two doses and reconstituted by tail vein injection of 4x10^6 bone marrow cells. Cells were a 50:50 mix of B6.Ly5.1 WT ($CD45.1^+$) and STAT6$^{-/-}$ ($CD45.2^+$) bone marrow. Mice were allowed to reconstitute for 6 weeks prior to use. Expression of CD45.1 or CD45.2 was used to distinguish WT and STAT6$^{-/-}$ cells from the same animal for analysis.

Cell isolation. Mice were anesthetized with isoflurane. Mice were perfused with PBS through the left ventricle. Draining lymph nodes and spleens were isolated, and a single-cell suspension was generated by passing cells through a 70-μm mesh filter. For collection of CNS mononuclear cells, brains were dissected from the skull, and spinal cords were flushed from the spinal column with PBS. Tissues were homogenized with an 18G needle and syringe in a solution containing 1 mg/ml collagenase A (Roche) and 1 mg/ml DNase 1 (Sigma-Aldrich) in HBSS and incubated at 37°C for 20 minutes. Mononuclear cells were separated from myelin with a 27% Percoll gradient (GE Healthcare).

Flow cytometry. Mononuclear cells were labelled with fixable viability dye (eFluor506 or eFluor780, eBioscience), blocked with anti-CD16/32 (Clone 2.4G2, hybridoma), and stained with fluorescent antibodies. For intracellular staining, cells were fixed with 4% paraformaldehyde, permeabilized with 0.5% saponin, and stained with fluorescent antibodies. Antibodies for CD62L (Clone MEL-14) and Ly6G (Clone 1A8) were obtained from BD Biosciences. The following antibodies were obtained from eBioscience: CD45 (Clone 30-F11), CD11b (Clone M1/70), CD11c (Clone N418), NOS2 (Clone CXNFT), CD44 (Clone IM7), CD4 (Clones RM4-5, GK1.5), MHC-II (Clone AF6-120.1), CD40 (Clone HM40-3), CD80 (Clone 16-10A1), CD86 (Clone GL1). Antibodies were conjugated to FITC, PE, PeCy7, APC, APC-Cy7, PerCP-Cy5.5, PerCP-eFluor710, PE/Dazzle 594, eFluor450, or PE-eFluor610. Arginase was stained with FITC-conjugated antibody (IC5868F, R&D Systems) or with unconjugated antibody (AF5858, R&D Systems) and an AlexaFluor 647-conjugated donkey anti-sheep secondary (ThermoFisher). Data was acquired using a FACSCanto II flow cytometer or FACSAria III flow sorter (BD Biosciences) and analyzed with FlowJo software (Treestar). Cells were sorted with a FACSAria III flow sorter (BD Biosciences).

Quantitative real-time PCR. Sorted cells were resuspended in RLT buffer, and RNA was isolated with the RNeasy Mini Kit (Qiagen). cDNA was generated by reverse transcription with the High Capacity cDNA Reverse Transcription Kit (Life Technologies). Quantitative real-time PCR (qRT-PCR) was performed on an iQ Thermocycler (Bio-Rad) using the iQ SYBR Green Supermix. Relative gene expression was determined with the ΔCT method with normalization to *Actb*.

Ex vivo cultures. For purification of naïve $CD4^+$ T cells, lymph nodes and spleen were collected from naïve 2D2 TCR transgenic mice, and $CD4^+$ T cells were enriched by positive selection with magnetic beads (Miltenyi). To further isolate naïve T cells, cells were sorted for live $CD4^+CD44^-CD62L^+$ T cells. For purification of memory T cells, mononuclear cells from the CNS were flow sorted for live $CD45^+CD11b^-CD3^+CD4^+$MHC-II^- T cells. T cells were labeled with CFSE according the manufacturer's instructions (ThermoFisher). Myeloid cell populations were sorted with markers as indicated in the text. Myeloid cells and T cells were co-cultured for 96 hours at a ratio of 1:20 (typically 5,000 myeloid cells with 95,000 T cells) in the presence or absence of myelin antigen (MOG_{35-55} peptide [Biosynthesis]).

Multiplex immunoassays. Cell culture supernatants were analyzed with the Milliplex Mouse Th17 Cytokine Panel (EMD Millipore) using the Bio-Plex 200 System (Bio-Rad). Values below the reported level of detection of the assay (minDC) were assigned a value of 0.5*minDC for statistical analysis and represented on graphs as not detectable (n.d.).

Immunohistochemistry on MS brain tissue. Human CNS tissue was obtained at autopsy according to an Institutional Review Board-approved protocol at Yale University. CNS tissue was obtained from 4 subjects with MS and a total of 5 chronic active white matter lesions were examined. Lesions were identified as "chronic active" according to the classification proposed by Bruce Trapp[37]. Specifically, lesions were characterized by ongoing demyelination at the lesion rim, with dense infiltration of CD68-positive myeloid cells that contained myelin degradation products. The lesion center was demyelinated but still contained lipid-positive myeloid cells. Post mortem intervals were between 5.5 and 24 hrs. Brain tissue was fixed with 10% formalin for 2 to 4 weeks and embedded in paraffin. Formalin-fixed, paraffin-embedded (FFPE) sections were cut, quenched with hydrogen peroxide and blocked with normal serum, incubated with primary antibodies overnight and finally processed with the appropriate biotinylated secondary antibody and avidin/biotin staining kit with diaminobenzidene as chromogen (Vector ABC Elite Kit and DAB Kit, Vector Laboratories), and counterstained with haematoxylin. The following antibodies were used in this study: MBP (Rabbit polyclonal, Dako A0623), CD68 (Mouse monoclonal, Dako M0876), iNOS (Rabbit polyclonal, Novus NB 120-15203), CD206 (Mouse polyclonal, Abcam ab117644), and Iba-1 (Goat polyclonal, Abcam ab5076). Adequate

controls using isotype control antibodies were performed with each primary antibody. Brightfield images were acquired with a Leica DM5000 B microscope using a Leica colour camera DFC310 Fx and the Leica Application Suite (version 4.2.0) imaging software. For fluorescence images, sections were incubated with fluorescent-labelled secondary antibodies and subsequently treated with 0.7% Sudan Black in ethanol and $CuSO_4$ to quench auto- fluorescence. Sections were counterstained with DAPI and mounted with VectaShield mounting medium (VectaShield Kit, Vector Laboratories). Images were acquired with an UltraVIEW VoX (Perkin Elmer) spinning disc confocal Nikon Ti-E Eclipse microscope. Image acquisition, visualization and quantification were performed using the Volocity 6.3 soft- ware (Improvision). Images were processed with the ImageJ software (Schneider et al., 2012). For 3D Surface plots, colors were split into red, green and blue, and only the red color images were processed further. Background was removed by setting an appropriate threshold and the resulting image was processed with the “Interactive Surface Plot v2.4” ImageJ plug-in.

Statistics. Statistical analysis was performed using paired or un-paired, 2-tailed Student’s t test, as indicated in the legends.

RESULTS

Macrophage polarization shifts from the core to the rim of MS lesions

In order to characterize the polarization state of $CD68^+$ macrophage in chronic active MS lesions, we immunolabelled brain tissue sections from 4 patients (Table 1) with antibodies against iNOS and CD206, the standard markers of classically and alternatively activated human myeloid cells, respectively[2,14,38,39]. MS lesions tend to grow centrifugally over time, with inflammatory activity gradually moving outward. Chronic active lesions have a relatively quiescent and hypocellular lesion center, due to waning of the earlier inflammatory response, surrounded by a rim of macrophages with early myelin degradation products, signifying ongoing demyelination[37]. We found that a high percentage of $CD68^+$ macrophages at the lesion rim were $iNOS^+$, while relatively few macrophages expressed CD206 (Figure 1A-D). Conversely, the ratio of $CD206^+$ cells was higher than $iNOS^+$ cells among those macrophages in the center of the lesion. We detected iNOS/CD206 double positive macrophages in all 5 MS lesions, which were most numerous in the lesion center (Figure 1E). Consistent with our results, Vogel and colleagues discovered foamy macrophages and activated microglia in a panel of active MS lesions that consistently co-expressed AAMC and CAMC markers[2].

Arg1 is expressed by a subset of CNS-infiltrating myeloid cells at peak EAE

Next, we investigated the phenotypes of CNS myeloid cells during the course of EAE. We found that the myeloid cells that accumulate in the CNS do not reliably express CD206 at onset, peak, or late time points of EAE, but a subset of splenic myeloid cells inconsistently expressed CD206 at high levels (data not shown). Since Arg1 is commonly used to identify murine AAMC[12], we measured expression of iNOS and Arg1 in inflammatory cells isolated from the spinal cord at serial time points following active immunization with myelin peptide. We detected iNOS, but not Arg1, in mononuclear cells isolated from the spinal cord at clinical onset (Figure 2A). In contrast, at peak disease we detected Arg1, but not iNOS, in the CNS myeloid cells. Arg1 was expressed by $CD45^{hi}CD11b^+$ infiltrating myeloid cells and $CD45^{int}CD11b^{int}$ resident microglia, but not by $CD45^+CD11b^-$ lymphoid cells or $CD45^-$ nonhematopoietic cells (Figure 2B). The $CD45^{hi}CD11b^+$ myeloid subset was further divided into $Ly6G^+$ neutrophils, $CD11c^-$ monocytes/ macrophages (MΦ), and $CD11c^+$

dendritic cells (DC). Arg1 was expressed by a significant percent of the infiltrating MΦ and DC, but not by neutrophils. At clinical onset, expression of iNOS followed a similar pattern both in spinal cord and brain mononuclear cells (data not shown). $Arg1^+$ and $iNOS^+$ myeloid cells were restricted to the CNS as no $Arg1^+$ or $iNOS^+$ cells were detected in the spleen, draining lymph nodes or blood (data not shown).

We sorted $Arg1^+$ and $Arg1^-$ MΦ ($CD45^{hi}CD11b^+Ly6G^-CD11c^-$) or DC ($CD45^{hi}CD11b^+Ly6G^-CD11c^+$) from the CNS of Arg1-eYFP reporter mice[35] during peak stage EAE, and we measured the expression of candidate genes by quantitative RT-PCR. Genes associated with *in vitro* generated AAMC, including Ym1 and Mrc1, were enriched in $Arg1^+$ CNS DC and MΦ, compared with their $Arg1^-$ counterparts, while CAMC-related genes (iNOS, IL-1β, IL-6) were unchanged or reduced (Figure 2C). The genetic profiles of $Arg1^+$ and $Arg1^-$ CNS myeloid cells did not precisely mirror those of *in vitro* generated AAMC and CAMC, respectively. For example, mRNA encoding the AAMC-associated cytokines IL-10 and TGFβ1 were expressed at similar levels $Arg1^-$ and $Arg1^+$ cells, and the CAMC-associated cytokine TNFα was expressed at relatively high levels in the $CD11c^-Arg1^+$ cohort. Reminiscent of these results, an $Arg1^+$ CNS myeloid subset with a mixed gene profile was recently described in traumatic brain injury[40], which may signify a distinct myeloid cell phenotype induced within the CNS microenvironment.

$Arg1^+$ myeloid cells accumulate in the CNS independent of STAT6

STAT6 has been identified as a critical regulator of Arg1 expression in BMDMs in response to IL-4 and IL-13 *in vitro*[41]. To determine whether STAT6 is also critical for the accumulation of $Arg1^+$ CNS myeloid cells during EAE, we constructed mixed bone marrow chimeric mice by reconstituting lethally irradiated WT mice with a combination of $STAT6^{-/-}$ and WT bone marrow cells. Brain and spinal cord mononuclear cells were isolated from individual chimeric mice at peak EAE for flow cytometric analysis. The frequency of $Arg1^+$ cells was modestly reduced among $STAT6^{-/-}$, compared with WT, myeloid cells isolated from the same CNS tissue (Figure 2D). Nonetheless, the accumulation of $Arg1^+$ CNS myeloid cells was largely preserved in the absence of STAT6.

Myeloid cells shift from iNOS to Arg1 expression during the evolution of adoptively transferred and relapsing remitting EAE

Active immunization involves the administration of CFA and pertussis toxin which could directly modulate innate immune cells. In order to determine how iNOS and Arg1 expression evolves in CNS myeloid cells during EAE in the absence of adjuvant, we utilized an adoptive transfer model. Naïve C57BL/6 mice were injected with myelin-primed syngeneic Th17 cells, and CNS mononuclear cells were isolated at serial time points for analysis by flow cytometry. Similar to our observations in the active immunization model, $iNOS^{+}Arg1^{-}$ cells were prominent during the preclinical stage and at clinical onset, while $iNOS^{-}Arg1^{+}$ cells were prominent during peak and late disease (Figure 3A). A population of $iNOS^{+}Arg1^{+}$ CNS myeloid cells also emerged at clinical onset but had contracted by peak EAE. This dynamic shift in the expression of iNOS and Arg1 occurred in CNS-infiltrating MΦ and DC, as well as in $CD45^{int}CD11b^{int}$ resident microglia (Figure 3B).

Next, we used a relapsing remitting model of EAE in SJL mice to determine whether myeloid cells undergo cyclical shifts in iNOS and Arg1 expression through multiple relapses. We observed that an $iNOS^{+}Arg1^{-}$ subset accumulated immediately prior to the first exacerbation, contracted during peak disease, and rebounded at relapse (Figure 3C-E). In contrast, an $iNOS^{-}Arg1^{+}$ subset expanded between the preclinical stage and peak EAE, waned during remission, and re-emerged at the peak of relapse. Collectively, these results demonstrate that a shift in myeloid cell phenotype parallels clinical exacerbations and remissions/ plateaus and is consistent across multiple models of EAE.

Individual myeloid cells convert from iNOS to Arg1 expression

Khoury and colleagues described immunosuppressive $Ly6C^{hi}$ monocytes that expand in the periphery, accumulate in the CNS during EAE, and have the potential to differentiate into either $iNOS^{+}$ or $Arg1^{+}$ cells upon *ex vivo* culture with different polarizing factors[20]. As shown in Figures 1 and 3, we detected myeloid cells in MS and EAE lesions that co-express AAMC and CAMC markers. It is unclear if these cells represent a distinct, stable lineage or an intermediate stage during the transition between polarized subsets. The experiments in Figures 3 demonstrate the evolving characteristics of CNS myeloid cells on a population level; however, they do not address plasticity at the level of individual cells. To this end, we permanently labelled $iNOS^{+}$ cells and their descendants by crossing NOS2-TdTomato-Cre reporter mice[36] with Rosa26-LSL-eYFP reporter mice to generate iNOS fate-mapping mice ($iNOS^{FM}$). Disease was induced in these mice by

adoptive transfer of myelin-primed Th17 cells. A subset of myeloid cells isolated from the CNS of the fate mapping mice at peak EAE expressed eYFP, indicative of previous expression of iNOS (iNOS^{FM+}) (Figure 4A-B). At this point, iNOS protein is no longer detectable. Approximately 45% of the iNOS^{FM+} subset co-expressed Arg1 (Figure 4C), demonstrating that individual CNS-infiltrating myeloid cells are capable of transitioning from expression of iNOS to expression of Arg1 during the course of disease. However, Arg1 expression is not absolutely dependent on prior expression of iNOS since ~15% of the iNOS^{FM-} cells were also Arg1^{+}. Notably, a higher percentage of Arg1^{+} than Arg1^{-} cells were derived from iNOS^{FM+} precursors (33% versus 9%). These data demonstrate that Arg1-expressing cells may be derived from iNOS-expressing cells or from iNOS-naïve cells.

Arg1-expressing CNS myeloid cells are inefficient antigen presenting cells

DCs have been identified as potent antigen presenting cells (APC) in the CNS during EAE[7,42]. We sought to compare the APC function of Arg1^{+} versus Arg1^{-} CNS DC by measuring the ability of each subset to promote myelin-specific T cell proliferation *ex vivo*. Sorted CNS DC subsets were co-cultured with naïve 2D2 CD4^{+} T cells, which bear a transgenic T cell receptor specific for myelin oligodendrocyte glycoprotein peptide (MOG_{35-55}), in the presence of myelin peptide. Compared with their Arg1^{-} counterparts, Arg1^{+} CNS DC were inefficient in promoting the proliferation of, or cytokine production by, myelin-specific T cells (Figure 5A-B). Similar results were obtained when MOG_{1-125} protein was used as the recall antigen (data not shown). The majority of CD4^{+} T cells within the CNS during EAE are CD44^{+}CD62L^{lo} effector cells. In order to simulate antigen presentation within the CNS more closely, we next isolated CD4^{+} effector T cells from the spinal cords of mice at peak EAE and co-cultured them with Arg1^{+} or Arg1^{-} CNS DC. Similar to naïve 2D2 T cells, the CD4^{+} effector T cells proliferated and secreted cytokines at reduced levels in response to antigen presentation by Arg1^{+} versus Arg1^{-} CNS DC (Figure 5C-D). The poor APC capacity of Arg1^{+} CNS DC did not appear to be due to low expression of MHC-II or co-stimulatory molecules (Figure 5E-F). Essentially all of the Arg1^{+} and Arg1^{-} CNS DC expressed MHC-II, though Arg1^{+} cells expressed a slightly lower level than their Arg1^{-} counterparts. Arg1^{+} CNS DC expressed similar levels of the co-stimulatory marker CD40 and slightly higher levels of CD80 and CD86 compared with Arg1^{-} CNS DC. Arginase enzyme activity has been shown to

suppress T cell proliferation in other experimental systems[43,44]; however, inhibition of arginase during co-cultures of T cells with $Arg1^+$ CNS myeloid cells did not rescue T cell activation (data not shown).

We next investigated whether $Arg1^+$ CNS myeloid cells are immunosuppressive or simply incompetent APCs. $Arg1^+$ CNS myeloid cells did not induce 2D2 T cells to upregulate FoxP3 (data not shown) or to produce IL-10 (Figures 5B, D). Furthermore, the addition of $Arg1^+$ CNS myeloid cells to co-cultures of $Arg1^-$ myeloid cells and 2D2 T cells did not impede antigen presentation by the $Arg1^-$ cells (data not shown). Hence, we concluded that $Arg1^+$ cells are intrinsically poor APC but do not actively block T cell activation by competent APC.

DISCUSSION

Collectively, the data presented in our study demonstrate the heterogeneity and plasticity of myeloid cells within the CNS in MS and EAE. We identified an $Arg1^+$ CNS myeloid population during the peak and later stages of EAE which is deficient in the capacity to activate myelin-specific T cells. The appearance of $Arg1^+$ myeloid cells in the CNS immediately prior to disease remission was consistent across multiple disease induction methods (active and adoptive) as well as across mouse strains (C57Bl/6 and SJL). CNS $Arg1^+$ DC were not immunosuppressive in the sense that they did not actively suppress T cell activation by their immunocompetent $Arg1^-$ counterparts. Nevertheless, the poor antigen presenting ability of these myeloid cells may passively contribute to the resolution of inflammation, and hence to clinical remission, following peak disease. The mechanism underlying ineffective antigen presentation by CNS $Arg1^+$ myeloid cells remains to be elucidated. We are currently interrogating the efficiency of myelin antigen loading on MHC-II molecules in CNS DC subsets. It is also possible that the $Arg1^+$ cells play an immunoregulatory or pro-regenerative role independent of T cell activation. Although the $Arg1^+$ cells do not produce IL-10 and express comparable levels of TGFβ1 to $Arg1^-$ cells, we are currently investigating whether they secrete other regulatory molecules. CNS AAMC may play a role in ameliorating the clinical course by clearing debris[23,24] and/or releasing trophic factors[25].

$Arg1^+$ CNS myeloid cells differ from *in vitro* polarized AAMC in that they differentiate in the absence of STAT6, express low levels of CD206 and high levels of MHC-II, and have a distinct genetic profile. The factors that drive their polarization *in vivo* are a subject of ongoing research. Candidates include HIF1α and PPARγ, which have been shown to promote AAMC differentiation in other experimental systems[45,46]. Alternatively, studies with primary human macrophages suggest that ingestion of myelin could trigger their development[19]. Unexpectedly, we found that the $Arg1^+$ CNS myeloid cells that accumulate in the CNS during EAE are derived, in part, from $iNOS^+$ precursors. Although plasticity of CAMC and AAMC has previously been demonstrated in other experimental systems on the population level, the current study is the first to our knowledge to directly demonstrate the transition of CNS myeloid cells from iNOS to Arg1 expression *in vivo* on the single cell level. Furthermore, during the transition from iNOS to Arg1 expression, CNS myeloid cells entered an intermediary stage characterized by expression of both markers. The demonstration by us and

others[2] that myeloid cells in MS lesions also co-express CAMC and AAMC markers raises the possibility that they undergo a dynamic transformation from a pro- to a non-inflammatory state. Such a transformation is further suggested by the increasing gradient of iNOS versus CD206 expression in macrophages extending from the active rim to the quiescent center of chronic active MS lesions.

Second generation disease modifying therapies (DMT) in MS suppress clinical exacerbations by depleting peripheral lymphocytes or blocking their trafficking to the CNS. While these reagents are highly effective in many individuals with relapsing-remitting MS, they are not cures, with up to 30% non-response rates. Furthermore, DMT currently used in the clinic are generally ineffective in progressive forms of MS. Myeloid cells and related factors have been under-utilized as candidate therapeutic targets in MS clinical trials. This is particularly relevant to secondary progressive MS, since numerous studies point to dysregulation of the innate arm of the immune system and, in particular, cells of the myeloid lineage as a distinctive feature of that stage of disease[47–50]. The current findings suggest an opportunity for slowing, or even halting, progressive disability in patients with MS via the development of novel therapeutics that suppress pathogenic myeloid subsets in a targeted manner and/or promote their conversion to a non-inflammatory phenotype.

ACKNOWLEDGEMENTS

This work was supported by NIH grants R01 NS057670 (to BMS), Training Grant 5T32GM7863-34 (to DAG), and Veterans Administration Merit Review Awards 1I01RX000416 and 1I01BX001387 (to BMS). BMS is a Scholar of the A. Alfred Taubman Medical Research Institute.

AUTHOR CONTRIBUTIONS

D.A.G., P.C.D., and B.M.S. contributed to study concept and design. D.A.G., J.M.W.S., S.D., G.P., and D.P. contributed to data acquisition and analysis. D.A.G. and B.M.S. contributed to drafting the manuscript and figures.

POTENTIAL CONFLICTS OF INTEREST

Nothing to report.

REFERENCES

1. Sobel RA, Blanchette BW, Bhan AK, Colvin RB. The immunopathology of experimental allergic encephalomyelitis. I. Quantitative analysis of inflammatory cells in situ. J. Immunol. 1984;132(5):2393–2401.

2. Vogel DY, Vereyken EJ, Glim JE, et al. Macrophages in inflammatory multiple sclerosis lesions have an intermediate activation status. J. Neuroinflammation 2013;10(1):35.

3. Deshpande P, King IL, Segal BM. Cutting Edge: CNS CD11c+ Cells from Mice with Encephalomyelitis Polarize Th17 cells and Support CD25+CD4+ T cell-Mediated Immunosuppression, Suggesting Dual Roles in the Disease Process. J. Immunol. 2007;178(11):6695–6699.

4. King IL, Dickendesher TL, Segal BM. Circulating Ly-6C+ myeloid precursors migrate to the CNS and play a pathogenic role during autoimmune demyelinating disease. Blood 2009;113(14):3190–3197.

5. Ajami B, Bennett JL, Krieger C, et al. Infiltrating monocytes trigger EAE progression, but do not contribute to the resident microglia pool. Nat. Neurosci. 2011;14(9):1142–1149.

6. Fife BT, Huffnagle GB, Kuziel WA, Karpus WJ. Cc Chemokine Receptor 2 Is Critical for Induction of Experimental Autoimmune Encephalomyelitis. J. Exp. Med. 2000;192(6):899–906.

7. Greter M, Heppner FL, Lemos MP, et al. Dendritic cells permit immune invasion of the CNS in an animal model of multiple sclerosis. Nat. Med. 2005;11(3):328–334.

8. Katz-Levy Y, Neville KL, Girvin AM, et al. Endogenous presentation of self myelin epitopes by CNS-resident APCs in Theiler's virus–infected mice. J. Clin. Invest. 1999;104(5):599–610.

9. Arango Duque G, Descoteaux A. Macrophage cytokines: involvement in immunity and infectious diseases. Front. Immunol. 2014;5:491.

10. Cross AH, Keeling RM, Goorha S, et al. Inducible nitric oxide synthase gene expression and enzyme activity correlate with disease activity in murine experimental autoimmune encephalomyelitis. J. Neuroimmunol. 1996;71(1–2):145–153.

11. Li S, Vana AC, Ribeiro R, Zhang Y. Distinct role of nitric oxide and peroxynitrite in mediating oligodendrocyte toxicity in culture and in experimental autoimmune encephalomyelitis. Neuroscience 2011;184:107–119.

12. Mills CD, Kincaid K, Alt JM, et al. M-1/M-2 Macrophages and the Th1/Th2 Paradigm. J. Immunol. 2000;164(12):6166–6173.

13. Wingerchuk DM, Lucchinetti CF, Noseworthy JH. Multiple sclerosis: current pathophysiological concepts. Lab. Investig. J. Tech. Methods Pathol. 2001;81(3):263–281.

14. De Groot CJ, Ruuls SR, Theeuwes JW, et al. Immunocytochemical characterization of the expression of inducible and constitutive isoforms of nitric oxide synthase in demyelinating multiple sclerosis lesions. J. Neuropathol. Exp. Neurol. 1997;56(1):10–20.

15. Nikić I, Merkler D, Sorbara C, et al. A reversible form of axon damage in experimental autoimmune encephalomyelitis and multiple sclerosis. Nat. Med. 2011;17(4):495–499.

16. Oleszak EL, Zaczynska E, Bhattacharjee M, et al. Inducible Nitric Oxide Synthase and Nitrotyrosine Are Found in Monocytes/Macrophages and/or Astrocytes in Acute, but Not in Chronic, Multiple Sclerosis. Clin. Diagn. Lab. Immunol. 1998;5(4):438–445.

17. Hill KE, Zollinger LV, Watt HE, et al. Inducible nitric oxide synthase in chronic active multiple sclerosis plaques: distribution, cellular expression and association with myelin damage. J. Neuroimmunol. 2004;151(1–2):171–179.

18. Fan X, Zhang H, Cheng Y, et al. Double Roles of Macrophages in Human Neuroimmune Diseases and Their Animal Models. Mediators Inflamm. 2016;2016:e8489251.

19. Boven LA, Meurs MV, Zwam MV, et al. Myelin-laden macrophages are anti-inflammatory, consistent with foam cells in multiple sclerosis. Brain 2006;129(2):517–526.

20. Zhu B, Bando Y, Xiao S, et al. CD11b+Ly-6Chi Suppressive Monocytes in Experimental Autoimmune Encephalomyelitis. J. Immunol. 2007;179(8):5228–5237.

21. Munder M. Arginase: an emerging key player in the mammalian immune system. Br. J. Pharmacol. 2009;158(3):638–651.

22. Stein M, Keshav S, Harris N, Gordon S. Interleukin 4 potently enhances murine macrophage mannose receptor activity: a marker of alternative immunologic macrophage activation. J. Exp. Med. 1992;176(1):287–292.

23. Kotter MR, Zhao C, van Rooijen N, Franklin RJM. Macrophage-depletion induced impairment of experimental CNS remyelination is associated with a reduced oligodendrocyte progenitor cell response and altered growth factor expression. Neurobiol. Dis. 2005;18(1):166–175.

24. Copelman CA, Diemel LT, Gveric D, et al. Myelin phagocytosis and remyelination of macrophage-enriched central nervous system aggregate cultures. J. Neurosci. Res. 2001;66(6):1173–1178.

25. Miron VE, Boyd A, Zhao J-W, et al. M2 microglia and macrophages drive oligodendrocyte differentiation during CNS remyelination. Nat. Neurosci. 2013;16(9):1211–1218.

26. Zhang Z, Zhang Z-Y, Schittenhelm J, et al. Parenchymal accumulation of CD163+ macrophages/microglia in multiple sclerosis brains. J. Neuroimmunol. 2011;237(1):73–79.

27. Wasser B, Pramanik G, Hess M, et al. Increase of Alternatively Activated Antigen Presenting Cells in Active Experimental Autoimmune Encephalomyelitis. J. Neuroimmune Pharmacol. 2016;1–12.

28. Xu L, Hilliard B, Carmody RJ, et al. Arginase and autoimmune inflammation in the central nervous system. Immunology 2003;110(1):141–148.

29. Zhang X-M, Lund H, Mia S, et al. Adoptive transfer of cytokine-induced immunomodulatory adult microglia attenuates experimental autoimmune encephalomyelitis in DBA/1 mice. Glia 2014;62(5):804–817.

30. Mikita J, Dubourdieu-Cassagno N, Deloire MS, et al. Altered M1/M2 activation patterns of monocytes in severe relapsing experimental rat model of multiple sclerosis. Amelioration of clinical status by M2 activated monocyte administration. Mult. Scler. J. 2011;17(1):2–15.

31. Benedek G, Zhang J, Bodhankar S, et al. Estrogen induces multiple regulatory B cell subtypes and promotes M2 microglia and neuroprotection during experimental autoimmune encephalomyelitis. J. Neuroimmunol. 2016;293:45–53.

32. Liu C, Li Y, Yu J, et al. Targeting the Shift from M1 to M2 Macrophages in Experimental Autoimmune Encephalomyelitis Mice Treated with Fasudil. PLoS ONE 2013;8(2):e54841.

33. Weber MS, Prod'homme T, Youssef S, et al. Type II monocytes modulate T cell–mediated central nervous system autoimmune disease. Nat. Med. 2007;13(8):935–943.

34. Kong W, Hooper KM, Ganea D. The natural dual cyclooxygenase and 5-lipoxygenase inhibitor flavocoxid is protective in EAE through effects on Th1/Th17 differentiation and macrophage/microglia activation. Brain. Behav. Immun. 2016;53:59–71.

35. Reese TA, Liang H-E, Tager AM, et al. Chitin induces accumulation in tissue of innate immune cells associated with allergy. Nature 2007;447(7140):92–96.

36. Béchade C, Colasse S, Diana MA, et al. NOS2 expression is restricted to neurons in the healthy brain but is triggered in microglia upon inflammation. Glia 2014;62(6):956–963.

37. Bö L, Mörk S, Kong PA, et al. Detection of MHC class II-antigens on macrophages and microglia, but not on astrocytes and endothelia in active multiple sclerosis lesions. J. Neuroimmunol. 1994;51(2):135–146.

38. Mehta V, Pei W, Yang G, et al. Iron Is a Sensitive Biomarker for Inflammation in Multiple Sclerosis Lesions. PLoS ONE 2013;8(3):e57573.

39. Lawrence T, Natoli G. Transcriptional regulation of macrophage polarization: enabling diversity with identity. Nat. Rev. Immunol. 2011;11(11):750–761.

40. Hsieh CL, Kim CC, Ryba BE, et al. Traumatic brain injury induces macrophage subsets in the brain. Eur. J. Immunol. 2013;43(8):2010–2022.

41. Gray MJ, Poljakovic M, Kepka-Lenhart D, Morris Jr. SM. Induction of arginase I transcription by IL-4 requires a composite DNA response element for STAT6 and C/EBPβ. Gene 2005;353(1):98–106.

42. Bailey SL, Schreiner B, McMahon EJ, Miller SD. CNS myeloid DCs presenting endogenous myelin peptides "preferentially" polarize CD4+ TH-17 cells in relapsing EAE. Nat. Immunol. 2007;8(2):172–180.

43. Rodriguez PC, Zea AH, Culotta KS, et al. Regulation of T Cell Receptor CD3ζ Chain Expression byl-Arginine. J. Biol. Chem. 2002;277(24):21123–21129.

44. Rodriguez PC, Zea AH, DeSalvo J, et al. l-Arginine Consumption by Macrophages Modulates the Expression of CD3ζ Chain in T Lymphocytes. J. Immunol. 2003;171(3):1232–1239.

45. Colegio OR, Chu N-Q, Szabo AL, et al. Functional polarization of tumour-associated macrophages by tumour-derived lactic acid. Nature 2014;513(7519):559–563.

46. Odegaard JI, Ricardo-Gonzalez RR, Goforth MH, et al. Macrophage-specific PPARγ controls alternative activation and improves insulin resistance. Nature 2007;447(7148):1116–1120.

47. Karni A, Abraham M, Monsonego A, et al. Innate Immunity in Multiple Sclerosis: Myeloid Dendritic Cells in Secondary Progressive Multiple Sclerosis Are Activated and Drive a Proinflammatory Immune Response. J. Immunol. 2006;177(6):4196–4202.

48. Segal BM. Stage-Specific Immune Dysregulation in Multiple Sclerosis. J. Interferon Cytokine Res. 2014;34(8):633–640.

49. Huber AK, Wang L, Han P, et al. Dysregulation of the IL-23/IL-17 axis and myeloid factors in secondary progressive MS. Neurology 2014;83(17):1500–1507.

50. Huber AK, Giles DA, Segal BM, Irani DN. An emerging role for eotaxins in neurodegenerative disease [Internet]. Clin. Immunol. 2016;Available from: http://www.sciencedirect.com/science/article/pii/S1521661616304004

FIGURE LEGENDS

Figure 1. CD206$^+$ and iNOS$^+$ macrophages are distributed from the center to the rim of active MS lesions. (A) Chronic active MS lesion immunolabeled for myelin basic protein (MBP) and CD68. (B) Cross sections of the same lesion, extending from the lesion center to the lesion rim, immunolabeled for CD206 and iNOS. (C) Quantification of iNOS$^+$ and CD206$^+$ cells at the lesion center and lesion rim. The number of cells is expressed as a percentage of CD68$^+$ cells. N=5 lesions quantified. *P<0.05, **P<0.01 by paired, 2-tailed Student's t test. (D) Surface plots of sections in B with the number of stained cells expressed as height, processed with the "Interactive Surface Plot v2.4" ImageJ plug-in. (E) Representative immunofluorescent labeling for CD206 (white), iNOS (magenta), and Iba1 (yellow). Scale bars indicate 150 μM (A); 100 μM (B) and 10 μM (E).

Figure 2. Arg1 expression defines a distinct myeloid cell population that accumulates in the CNS during later stages of EAE. (A, B) EAE was induced in mice by active immunization with myelin peptide. Inflammatory cells were isolated from the CNS at the onset or peak of clinical disability. Representative intracellular staining of Arg1 and iNOS in CNS immune cells from WT mice gating on (A) all viable cells at onset or peak or (B) cell subsets at peak disease. (C) Arg1$^+$ and Arg1$^-$ myeloid cells were flow sorted from the CNS of Arg1-eYFP reporter mice. M1 and M2 related transcripts were measured by qRT-PCR. Data are represented as the ratio of gene expression in Arg1$^+$ cells over Arg1$^-$ cells. (D) Inflammatory cells were isolated from the CNS of STAT6$^{-/-}$:WT→WT mixed bone marrow chimeric mice at the peak of EAE. Representative flow and quantification of intracellular staining of Arg1 and iNOS in WT or STAT6$^{-/-}$ cells, gated on the CD45^{hi}CD11b$^+$Ly6G$^-$ population. Percentages are Arg1$^+$ cells among WT or STAT6$^{-/-}$ CNS myeloid cells isolated from individual chimeric mice. Connected dots indicate cells derived from the same mouse. *P<0.05, **P<0.01, ***P<0.001 and n.s. = P>0.05, by paired, 2-tailed Student's t test. Data are representative of at least 2 experiments. N=3-5 mice per group. All values are mean ± SEM.

Figure 3. Myeloid cells shift from iNOS to Arg1 expression in adoptive transfer and relapsing models of EAE. (A, B) EAE was induced by adoptive transfer of WT myelin-primed Th17 cells into naïve syngeneic hosts. CNS inflammatory cells were isolated at serial time points and analyzed by flow cytometry. (A) Representative intracellular staining of Arg1 and iNOS, gating on the CD45^{hi}CD11b$^+$Ly6G$^-$ population. (B) Percentages of CD45^{hi}CD11b$^+$CD11c$^-$ MΦ, CD45^{hi}CD11b$^+$CD11c$^+$ DC and CD45^{mid}CD11b$^+$CD11c$^-$ microglia expressing iNOS and/or Arg1 in naïve mice (N) and in mice with EAE during the pre-clinical (PC), onset (O), peak (P), and late (L) stages of disease. (C-E) EAE was induced in SJL mice by active immunization with PLP$_{139-151}$ peptide, and CNS inflammatory cells were collected at serial time points, including onset (O), peak of first episode (P), remission (Rem), and relapse (Rel). Cells were also collected from mice that experienced an initial exacerbation followed by remission but did not subsequently relapse (No Rel). (C) Representative dot plots of intracellular iNOS and Arg1 expression gating on the CD45^{hi}CD11b$^+$Ly6G$^-$ population. (D) Representative relapsing-remitting clinical course of SJL mice. (E) Percentages of CD45^{hi}CD11b$^+$Ly6G$^-$ CNS myeloid cells expressing iNOS and/or Arg1 at serial time points. Data are representative of at least 2 experiments. N=3-5 mice per time point. All values are mean ± SEM.

Figure 4. Arg1-expressing CNS myeloid cells are derived, in part, from iNOS-expressing precursors. EAE was induced in mice by adoptive transfer of WT myelin-primed Th17 cells. CNS inflammatory cells were analyzed by flow cytometry. (A-C) Inflammatory cells were isolated from the spinal cords of iNOS^{FM} mice at peak disease. (A-B) Representative dot plots showing iNOS^{FM} and (A) Arg1 or (B) iNOS expression, gated on CD45^{hi}CD11b$^+$Ly6G$^-$ myeloid cells. (C) Percentages of CNS myeloid cell subpopulations defined according to iNOS^{FM} and Arg1 expression. Subpopulations were initially segregated based on expression of iNOS^{FM} (left) or Arg1 (right). Data are representative of at least 2 experiments. N=3-5 mice per group. Mean values are shown.

Figure 5. Arg1$^+$ cells are deficient at antigen presentation. EAE was induced in Arg1-eYFP reporter mice by active immunization with myelin peptide, and immune cells were isolated from the CNS at peak disease. Arg1$^+$ and Arg1$^-$ CD45^{hi}CD11b$^+$Ly6G$^-$CD11c$^+$ myeloid cells were flow sorted and co-cultured with MOG-reactive T cells in the presence of myelin peptide (MOG$_{35-55}$). (A-B) CNS myeloid cell subsets were co-cultured with CD44$^-$CD62L$^+$ CD4$^+$ T cells from naïve 2D2 TCR transgenic mice. (C, D) CNS myeloid subsets

were co-cultured with $CD4^+$ T cells isolated from the CNS of actively immunized WT mice at the peak of EAE. Graphs show (A, C) proliferation measured by CFSE dilution and (B, D) cytokine levels in culture supernatants, measured by multiplex bead assay. (E, F) MHC-II and co-stimulatory marker expression were measured by flow cytometry on $Arg1^+$ and $Arg1^-$ $CD45^{hi}CD11b^+Ly6G^-CD11c^+$ myeloid cells from the spinal cord at the peak of disease. (E) MHC-II expression quantified as both a percentage and by geometric MFI. (F) Co-stimulatory marker expression quantified by geometric MFI. *P<0.05, **P<0.01, and n.s. = P>0.05, by paired, 2-tailed Student's t test. Data are representative of at least 2 experiments. N=3-5 mice per group.

TABLES

Table 1: Clinical data of MS patients included in this study

Case	Age	Gender	Disease Course	Disease Duration	Post-mortem Interval
1	42	Male	RRMS	20 yrs	5.5 hrs
2	37	Male	RRMS	15 yrs	24 hrs
3	50	Female	RRMS	10 yrs	6 hrs
4	63	Female	SPMS	unknown	8 hrs

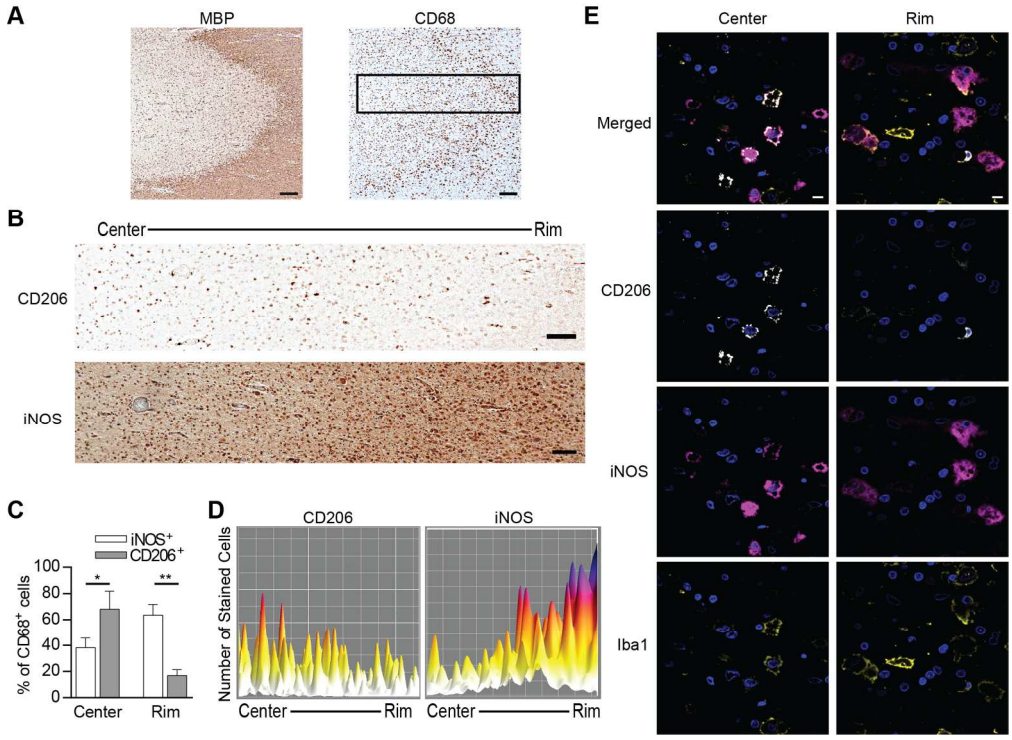

Figure 1. CD206+ and iNOS+ macrophages are distributed from the center to the rim of active MS lesions. (A) Chronic active MS lesion immunolabeled for myelin basic protein (MBP) and CD68. (B) Cross sections of the same lesion, extending from the lesion center to the lesion rim, immunolabeled for CD206 and iNOS. (C) Quantification of iNOS+ and CD206+ cells at the lesion center and lesion rim. The number of cells is expressed as a percentage of CD68+ cells. N=5 lesions quantified. *P<0.05, **P<0.01 by paired, 2-tailed Student's t test. (D) Surface plots of sections in B with the number of stained cells expressed as height, processed with the "Interactive Surface Plot v2.4" ImageJ plug-in. (E) Representative immunofluorescent labeling for CD206 (white), iNOS (magenta), and Iba1 (yellow). Scale bars indicate 150 μM (A); 100 μM (B) and 10 μM (E).

174x127mm (300 x 300 DPI)

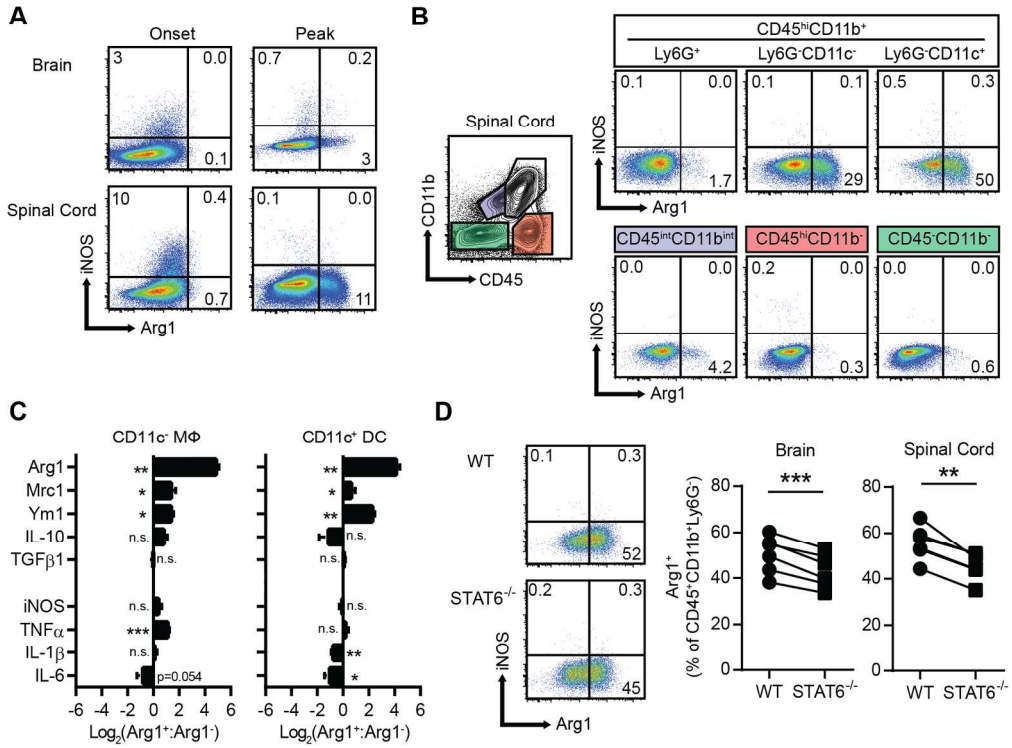

Figure 2. Arg1 expression defines a distinct myeloid cell population that accumulates in the CNS during later stages of EAE. (A, B) EAE was induced in mice by active immunization with myelin peptide. Inflammatory cells were isolated from the CNS at the onset or peak of clinical disability. Representative intracellular staining of Arg1 and iNOS in CNS immune cells from WT mice gating on (A) all viable cells at onset or peak or (B) cell subsets at peak disease. (C) Arg1+ and Arg1- myeloid cells were flow sorted from the CNS of Arg1-eYFP reporter mice. M1 and M2 related transcripts were measured by qRT-PCR. Data are represented as the ratio of gene expression in Arg1+ cells over Arg1- cells. (D) Inflammatory cells were isolated from the CNS of STAT6-/-:WT◊WT mixed bone marrow chimeric mice at the peak of EAE. Representative flow and quantification of intracellular staining of Arg1 and iNOS in WT or STAT6-/- cells, gated on the CD45hiCD11b+Ly6G- population. Percentages are Arg1+ cells among WT or STAT6-/- CNS myeloid cells isolated from individual chimeric mice. Connected dots indicate cells derived from the same mouse. *P<0.05, **P<0.01, ***P<0.001 and n.s. = P>0.05, by paired, 2-tailed Student's t test. Data are representative of at least 2 experiments. N=3-5 mice per group. All values are mean ± SEM.

164x136mm (300 x 300 DPI)

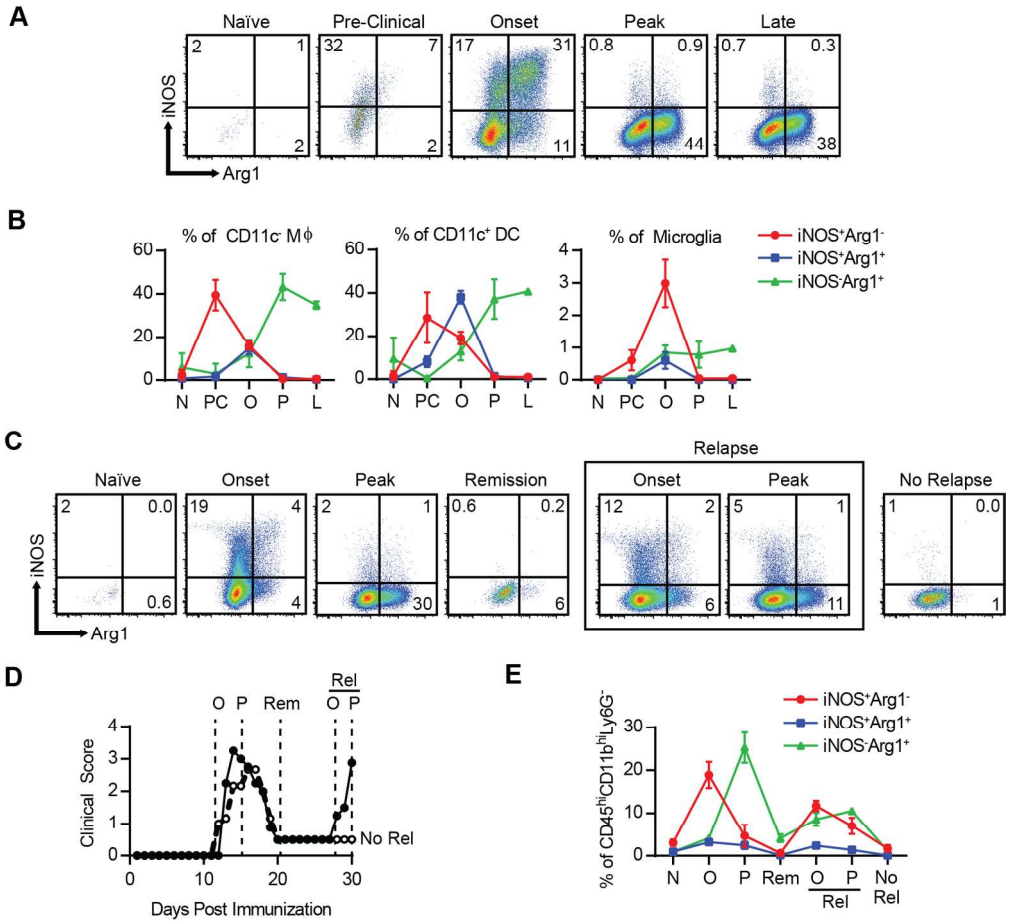

Figure 3. Myeloid cells shift from iNOS to Arg1 expression in adoptive transfer and relapsing models of EAE. (A, B) EAE was induced by adoptive transfer of WT myelin-primed Th17 cells into naïve syngeneic hosts. CNS inflammatory cells were isolated at serial time points and analyzed by flow cytometry. (A) Representative intracellular staining of Arg1 and iNOS, gating on the CD45hiCD11b+Ly6G- population. (B) Percentages of CD45hiCD11b+CD11c- MΦ, CD45hiCD11b+CD11c+ DC and CD45midCD11b+CD11c- microglia expressing iNOS and/or Arg1 in naïve mice (N) and in mice with EAE during the pre-clinical (PC), onset (O), peak (P), and late (L) stages of disease. (C-E) EAE was induced in SJL mice by active immunization with PLP139-151 peptide, and CNS inflammatory cells were collected at serial time points, including onset (O), peak of first episode (P), remission (Rem), and relapse (Rel). Cells were also collected from mice that experienced an initial exacerbation followed by remission but did not subsequently relapse (No Rel). (C) Representative dot plots of intracellular iNOS and Arg1 expression gating on the CD45hiCD11b+Ly6G- population. (D) Representative relapsing-remitting clinical course of SJL mice. (E) Percentages of CD45hiCD11b+Ly6G- CNS myeloid cells expressing iNOS and/or Arg1 at serial time points. Data are representative of at least 2 experiments. N=3-5 mice per time point. All values are mean ± SEM.

158x154mm (300 x 300 DPI)

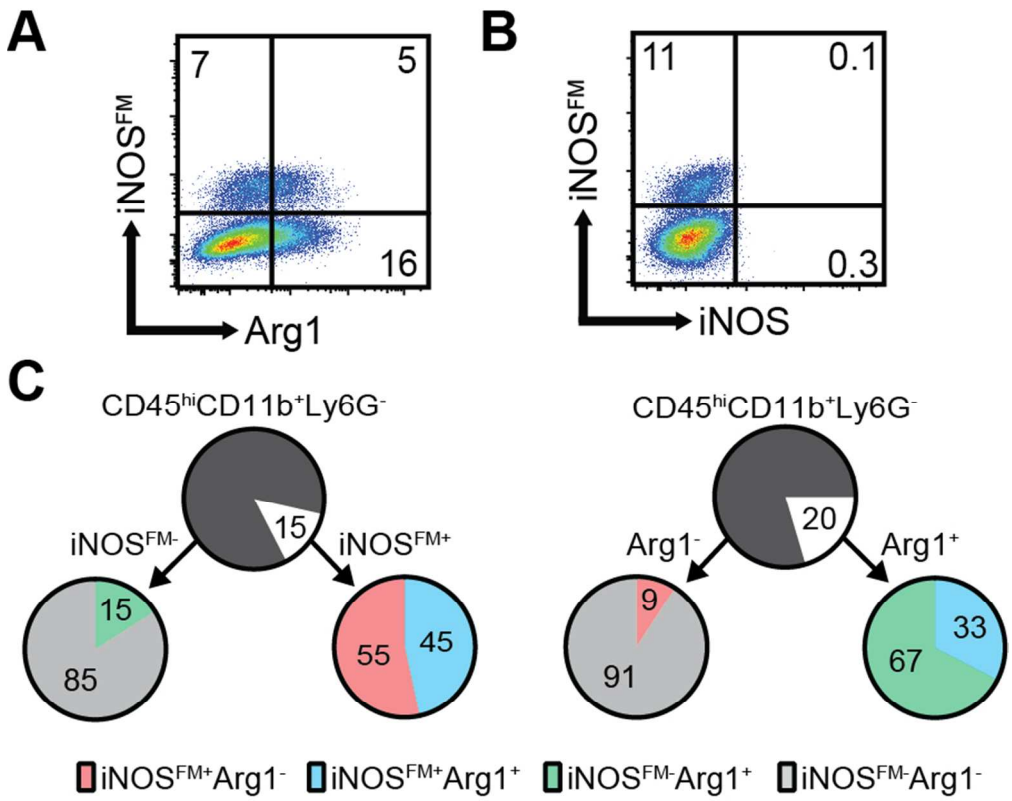

Figure 4. Arg1-expressing CNS myeloid cells are derived, in part, from iNOS-expressing precursors. EAE was induced in mice by adoptive transfer of WT myelin-primed Th17 cells. CNS inflammatory cells were analyzed by flow cytometry. (A-C) Inflammatory cells were isolated from the spinal cords of iNOSFM mice at peak disease. (A-B) Representative dot plots showing iNOSFM and (A) Arg1 or (B) iNOS expression, gated on CD45hiCD11b+Ly6G- myeloid cells. (C) Percentages of CNS myeloid cell subpopulations defined according to iNOSFM and Arg1 expression. Subpopulations were initially segregated based on expression of iNOSFM (left) or Arg1 (right). Data are representative of at least 2 experiments. N=3-5 mice per group. Mean values are shown.

76x60mm (300 x 300 DPI)

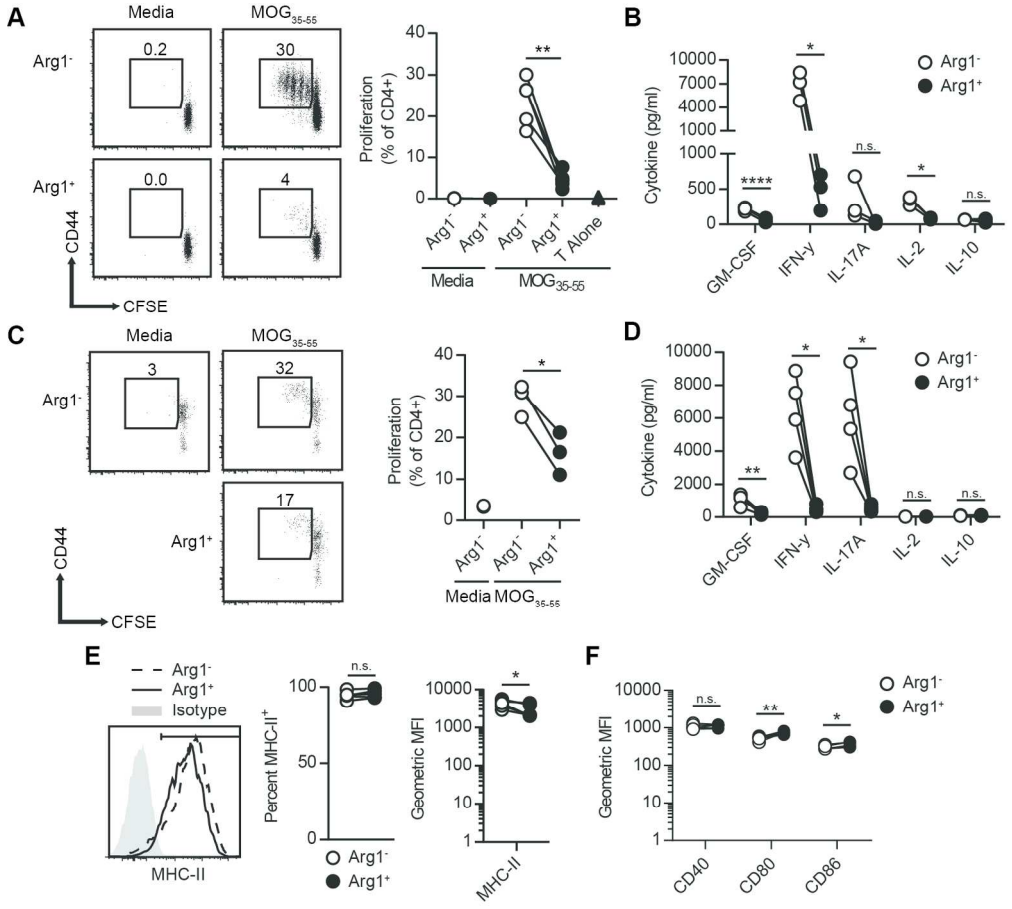

Figure 5. Arg1+ cells are deficient at antigen presentation. EAE was induced in Arg1-eYFP reporter mice by active immunization with myelin peptide, and immune cells were isolated from the CNS at peak disease. Arg1+ and Arg1- CD45hiCD11b+Ly6G-CD11c+ myeloid cells were flow sorted and co-cultured with MOG-reactive T cells in the presence of myelin peptide (MOG35-55). (A-B) CNS myeloid cell subsets were co-cultured with CD44-CD62L+ CD4+ T cells from naïve 2D2 TCR transgenic mice. (C, D) CNS myeloid subsets were co-cultured with CD4+ T cells isolated from the CNS of actively immunized WT mice at the peak of EAE. Graphs show (A, C) proliferation measured by CFSE dilution and (B, D) cytokine levels in culture supernatants, measured by multiplex bead assay. (E, F) MHC-II and co-stimulatory marker expression were measured by flow cytometry on Arg1+ and Arg1- CD45hiCD11b+Ly6G-CD11c+ myeloid cells from the spinal cord at the peak of disease. (E) MHC-II expression quantified as both a percentage and by geometric MFI. (F) Co-stimulatory marker expression quantified by geometric MFI. *P<0.05, **P<0.01, and n.s. = P>0.05, by paired, 2-tailed Student's t test. Data are representative of at least 2 experiments. N=3-5 mice per group.

165x149mm (300 x 300 DPI)

Table 1: Clinical data of MS patients included in this study					
Case	**Age**	**Gender**	**Disease Course**	**Disease duration**	**Post-mortem Interval**
1	42	Male	RRMS	20 yrs	5.5 hrs
2	37	Male	RRMS	15 yrs	24 hrs
3	50	Female	RRMS	10 yrs	6 hrs
4	63	Female	SPMS	unknown	8 hrs